First-Principles Calculations for Adsorption of HF, COF₂, and CS₂ on Pt-Doped Single-Walled Carbon Nanotubes

Zhengqin CAO, Xiaoyu WU, Gang WEI,* Gang HU, Qiang YAO, and Haiyan ZHANG

ACCESS | Metrics & More | Article Recommendations | SI Supporting Information

ABSTRACT: HF, CS₂, and COF₂ are three important decomposition components of the SF₆ gas insulation medium. In this paper, the gas sensitivity of Pt doped on (8, 0) single-walled carbon nanotube (SWCNT) to HF, CS₂, and COF₂ is investigated based on density functional theory. The binding energy, charge transfer, density of states, and frontier molecular orbital theory are discussed. It is found that all processes of HF, CS₂, and COF₂ adsorbed on Pt-SWCNT are exothermic. Pt-SWCNT donated 0.182 electrons to CS₂ molecules during the interaction process but acts as an electron acceptor during adsorption of HF and COF₂ on it. After comprehensive consideration of binding energy and charge transfer, the response of Pt- SWCNT to CS₂ may be the best, and those to HF and COF₂ are almost the same. In addition, after the adsorption of the three kinds of gases on Pt-SWCNT, the order of the conductivity of the Pt-SWCNT material is CS₂ > COF₂ ≈ HF via frontier molecular orbital theory analysis. The Pt-SWCNT material is probably more suitable as a gas sensor for the detection of CS₂ in the application of gas-insulated equipment.
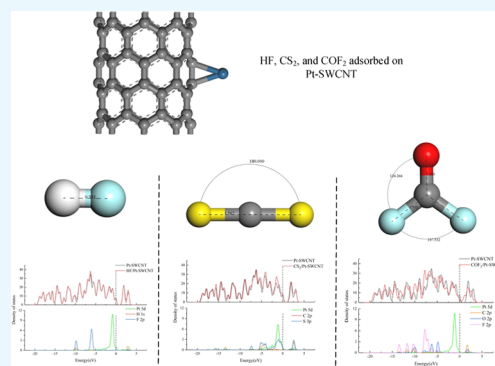
1. INTRODUCTION

SF₆ has been widely used as insulation medium for the operation safety of gas-insulated equipment due to its insulation and excellent arc extinguishing characteristics.[1−4] However, in long-running gas-insulated equipment, SF₆ would decompose in partial discharge to F atoms and other low fluorinated sulfur species, which further react with trace H₂O, trace O₂, and organic solid insulation material to generate HF, COF₂, CS₂, SO₂, SOF₂, SO₂F₂, S₂F₁₀, etc.[5−9] It has been proved that detecting SF₆ characteristic decomposed products by chemical sensors is a feasible and effective method to online monitoring and insulation defect diagnosis of gas-insulated equipment.[10−13]

In recent years, due to the strong responsivity, small size, and high sensitivity of a single-walled carbon nanotube (SWCNT),[14−16] it has been a research hotspot as a sensor material. Moreover, the gas sensitivity of the SWCNT will enhance after decorating its surface with transition metals[17−21] and realize its application to detect some gases.[22] Cui et al. found that the SWCNT doped with Pt, Pd, and Rh has good gas sensitivity to SOF₂, CO, CH₄, and H₂S, due to strong orbital interactions and chemisorption between the adsorbent and the target gas[10,23,24] by simulations. Yoosefian studied the adsorption properties of SO₂ on Pt- and Au-doped SWCNTs (5, 5) and found that the energy gap of SO₂ adsorbed on Pt-SWCNT changes more significantly than that on Au-SWCNT.[25]

There are a few studies about the gas-sensitive materials for HF, CS₂, and COF₂, which can more effectively represent the degree of solid insulator defects in SF₆ gas-insulated equipment, and Pt doped on the SWCNT surface is a promising material for gas sensor development. The adsorption properties of HF, CS₂,

and COF₂ adsorbing on Pt doped on (8, 0) SWCNT were calculated and analyzed based on density functional theory (DFT). The work provides fundamental adsorption information of Pt doped on (8, 0) SWCNT as a possible candidate for a chemical sensor applied in condition monitoring and defect diagnosis in SF₆ gas-insulated equipment.

2. COMPUTATION DETAILS

All of the calculations in the work were performed by the Dmol3 module based on DFT.[26,27] The atomic orbital basis sets adopted double numerical plus polarization (DNP).[28] The Perdew−Burke−Ernzerhof (PBE) generalized gradient approximation (GGA) was used to deal with electron exchange and correlation. The Brillouin zone k-point was sampled as $1 \times 1 \times 8$ from the Monkhorst−Pack mesh[10,29] with semicore pseudopots being adopted as the core treatment.[26] Maximum force, energy tolerance accuracy, and maximum atom displacement were selected as 0.002 Ha/Å, 1.0×10^{-5} Ha, and 5×10^{-3} Å, respectively.[16,30] The charge density convergence accuracy of the self-consistent field was 1.0×10^{-6} Ha.

All of the sizes of supercells were 20 Å × 20 Å × 8.50 Å with angles of $\alpha = 90°$, $\beta = 90°$, and $\gamma = 120°$. The initial HF
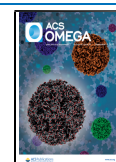
adsorption orientation includes two adsorption modes, namely, the H and F atoms approaching the Pt site of the Pt-SWCNT surface (as shown in Figure S1). For CS_2, the initial adsorption orientation includes two modes as well, namely, the C and S atoms approaching the Pt site of the Pt-SWCNT surface (as shown in Figure S2). Three modes, namely, the C, O, and F atoms approaching the Pt site of the Pt-SWCNT surface, were considered for the initial COF_2 adsorption orientation (as shown in Figure S3). Only the detailed analysis of the adsorption modes with the largest binding energy was discussed in this paper, including charge transfer, density of states (DOS), morphology, and frontier molecular orbital.

The binding energy E_{ad} represents the change of the gas molecule adsorption system and is given in formula (1)[31,32]

$$E_{ad} = E_{molecule/Pt-SWCNT} - E_{molecule} - E_{Pt-SWCNT} \qquad (1)$$

where $E_{molecule/Pt-SWCNT}$ represents the energy of the total system after adsorption of one gas molecule. $E_{molecule}$ and $E_{Pt-SWCNT}$ represent the energies of one gas molecule and the intrinsic Pt-SWCNT surface, respectively.

The charge transfer Q_t between Pt-SWCNT and gas molecules was estimated via Mulliken population analysis. If $Q_t < 0$, the electrons transfer from the Pt-SWCNT surface to gas molecules during the adsorption process, and the electrons transfer from gas molecules to the Pt-SWCNT surface when $Q_t > 0$.

3. RESULTS AND DISCUSSION

Before the adsorption calculation, the structures of HF, CS_2, COF_2, and Pt-SWCNT were optimized. SWCNT (8, 0) is
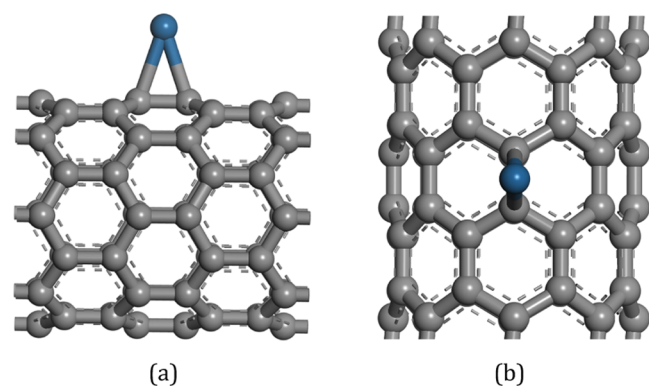
Figure 1. Optimized structure of Pt-SWCNT: (a) front view and (b) top view.

Table 1. Parameters of the Adsorption Configurations of HF, CS_2, and COF_2 on Pt-SWCNT

gas molecule	binding energy (eV)	charges transfer (e)	distance (Å)
HF	−0.325	0.045	2.268
CS_2	−1.037	−0.182	2.211
COF_2	−0.464	0.029	2.454

selected as the carrier, and the Pt atom is connected to two adjacent C atoms on the SWCNT, which forms a bridge site outside the SWCNT,[33] as shown in Figure 1. The bond lengths of both Pt and its adjacent two C atoms are 2.264 Å with a C−Pt−C angle of 36.996°. In addition, there is no deformation of the SWCNT after Pt doping.
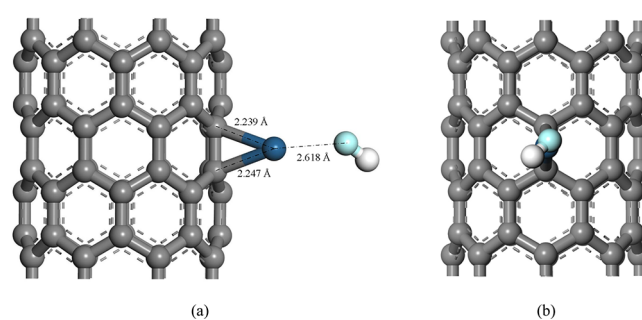
Figure 2. Adsorption configuration of HF on the Pt-SWCNT surface: (a) front view and (b) top view.
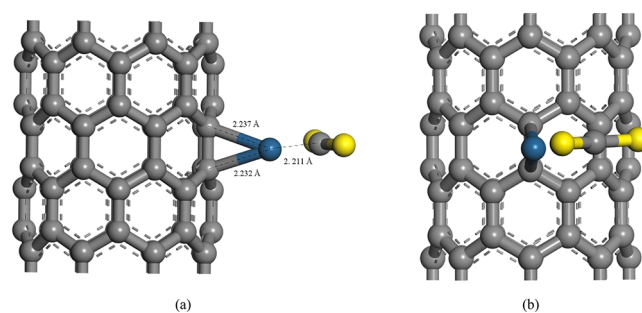
Figure 3. Adsorption configuration of CS_2 on the Pt-SWCNT surface: (a) front view and (b) top view.
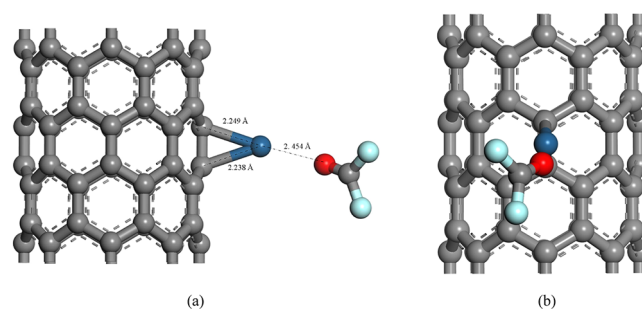
Figure 4. Adsorption configuration of COF_2 on the Pt-SWCNT surface: (a) front view and (b) top view.

The optimized structures and their parameters of HF, CS_2, and COF_2 molecules are shown in Figure S4.

3.1. Adsorption Configurations of HF, CS_2, and COF_2 on Pt-SWCNT. For all adsorption configurations of HF, CS_2, and COF_2 on the Pt-SWCNT surface, we only discuss the ones with the largest binding energy. The parameters of the adsorption configurations of the three gas molecules are listed in Table 1.

For HF, when the HF molecule is close to the Pt-SWCNT surface by the H atom, the largest binding energy is −0.325 eV in the two adsorption orientation modes. The adsorption configuration of HF is shown in Figure 2. The adsorption distance (between Pt and F) is 2.268 Å, and the bond lengths of Pt and its adjacent two C atoms change to 2.239 and 2.247 Å after adsorption, respectively. However, the structures of the SWCNT and the HF molecule have not changed during the adsorption process. In total, 0.045 electrons transfer from HF to the Pt-SWCNT surface, which indicates that HF acts as an electron donor.

The adsorption configuration of CS_2 is shown in Figure 3. The binding energy is −1.037 eV and the adsorption distance is 2.211
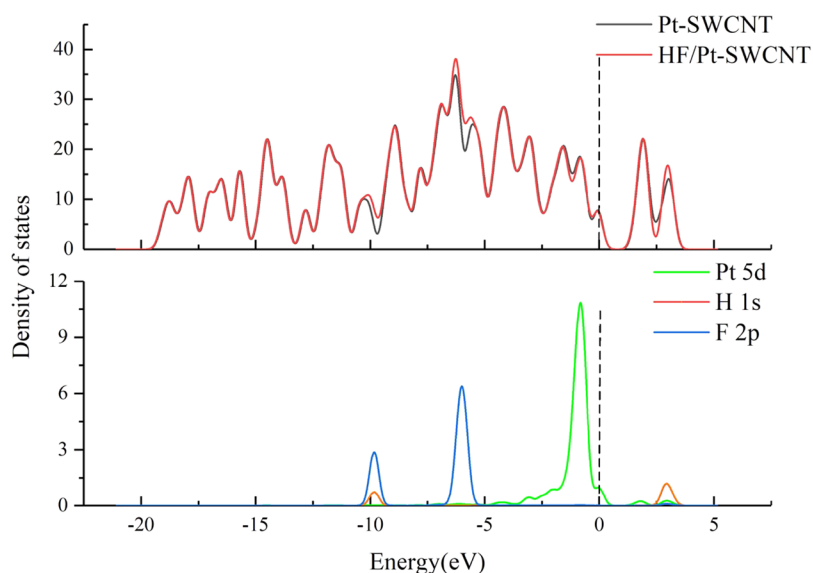
Figure 5. DOS distribution of HF adsorbed on the Pt-SWCNT surface.
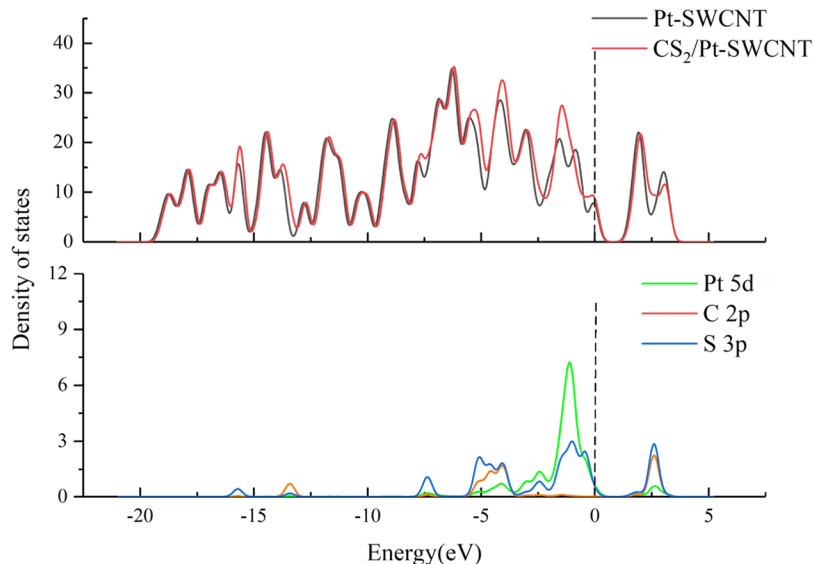
Figure 6. DOS distribution of CS_2 adsorbed on the Pt-SWCNT surface.

Å. Both C−S bond lengths of CS_2 increase from 1.567 to 1.593 Å and 1.636 Å, while the bond angle of C−S−C decrease from 180 to 156.845° after the adsorption. In addition, the bond lengths of Pt and its adjacent two C atoms decrease to 2.237 and 2.232 Å, respectively. The Pt-SWCNT surface donated 0.182 electrons to the CS_2 molecule.

Figure 4 exhibits the adsorption configuration of COF_2. The adsorption distance is 2.454 Å with a binding energy of −0.464 eV. The structure of COF_2 has changed slightly after adsorption. The bond lengths of Pt and its adjacent two C atoms decrease to 2.238 and 2.249 Å, respectively. In addition, the Pt-SWCNT surface obtains 0.029 electrons from the COF_2 molecule during the adsorption process.

Larger adsorption energy means a larger amount of gas could adsorb on the surface of a gas-sensing material.[34] Meanwhile, more charge transfer could give rise to higher sensitivity in the same adsorption condition.[35] Therefore, due to larger binding energy and charge transfer, Pt- SWCNT may have the best response to CS_2 among the three kinds of gas molecules.

However, due to the larger binding energy and the smaller charge transfer of the COF_2 system than those of the HF system, the response of Pt-SWCNT to COF_2 may be nearly the same as that to HF.

3.2. Density of States Analysis for HF, CS_2, and COF_2 Adsorbed on Pt-SWCNT. To further estimate the interaction mechanism between HF, CS_2, and COF_2 and Pt-SWCNT, the density of states (DOS) distributions of the three gas molecules on the Pt-SWCNT surface are discussed; 0 eV refers to the Fermi level. Figure 5 shows the total density of states (TDOS) and local density of states (LDOS) distribution of HF adsorbed on Pt-SWCNT. The TDOS increase little at the Fermi level but increase obviously at −9.8, −6.5, and −5.5 eV after HF adsorption. According to LDOS, the overlap between the 1s orbital of the H atom, the 2p orbital of the F atom, and the 5d orbital of the Pt atom is not significant, which indicates that the interaction between HF and the Pt-SWCNT surface is weak. In addition, the band gap decreases 0.010 eV after HF adsorption
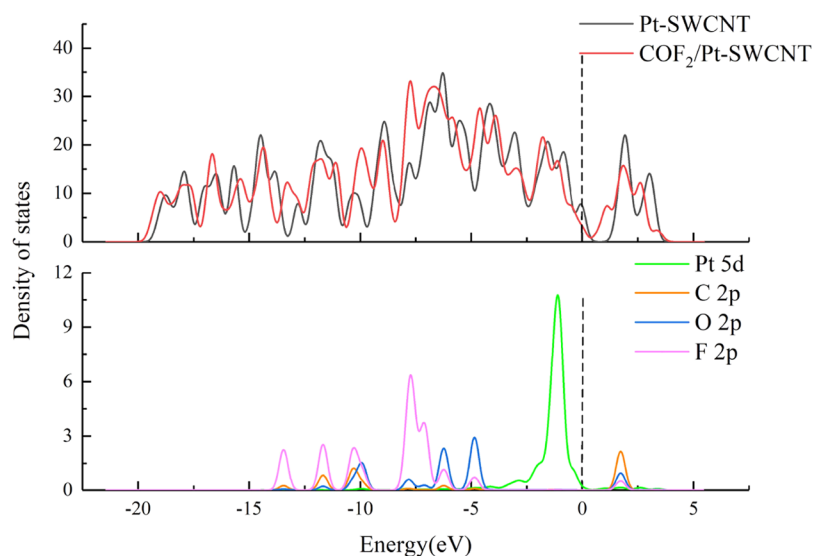
Figure 7. DOS distribution of COF_2 adsorbed on the Pt-SWCNT surface.

(a)

(b)
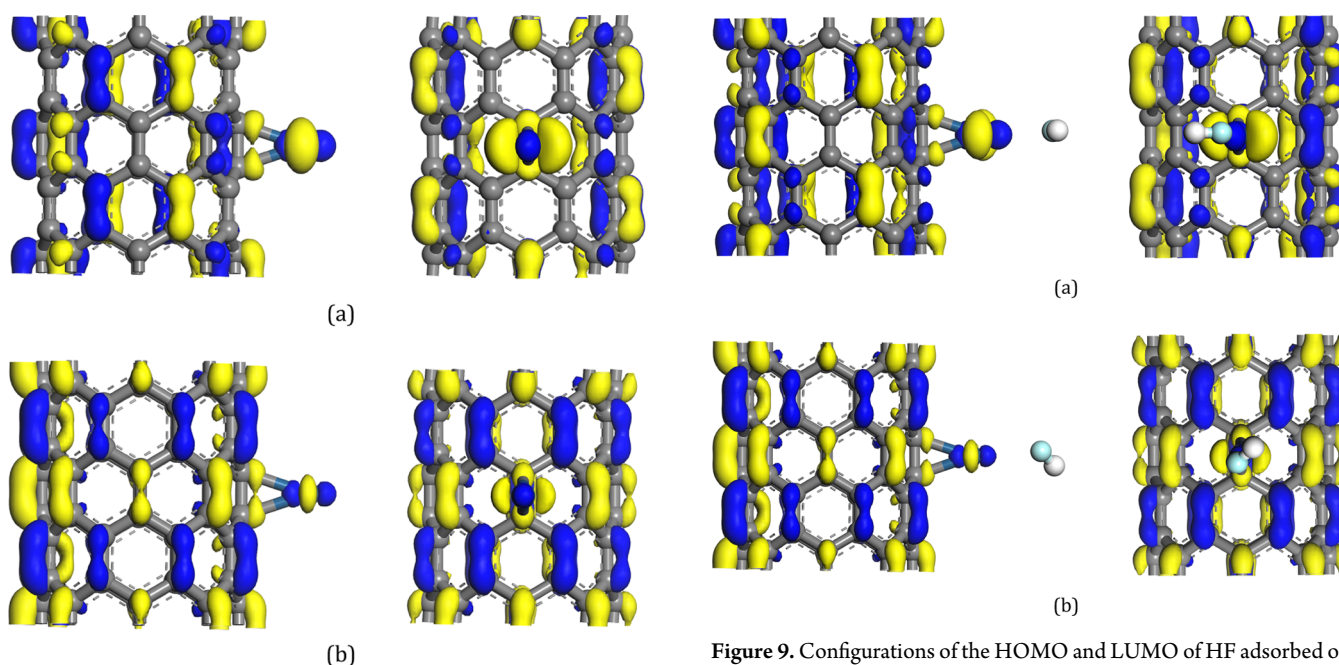
Figure 8. Configurations of the HOMO and LUMO of Pt-SWCNT with front and top view: (a) HOMO and (b) LUMO.

Table 2. Values of HOMO and LUMO

calculation system	LUMO (eV)	HOMO (eV)	E_g (eV)
Pt-SWCNT	−4.377	−5.084	0.747
HF/Pt-SWCNT	−4.288	−4.998	0.711
CS2/Pt-SWCNT	−4.612	−5.307	0.695
COF2/Pt-SWCNT	−4.283	−4.993	0.710

Figure 6 shows the DOS distribution of CS_2 adsorbed on the Pt-SWCNT surface. The TDOS increases at −15.8, −13, −7.5, −5, −4.2, −1.8, and 2.5 eV after CS_2 adsorption. Compared with LDOS distribution, the increased areas of the TDOS derive from the CS_2 molecule. In addition, the 3p orbital of the S atom and the 2p orbital of the C atom in CS_2 overlaps with the 5d orbital of Pt at −5.2 to 0 and 1.2−3.6 eV, respectively, indicating that the interaction between the CS_2 molecule and Pt-SWCNT is strong.

(a)

(b)
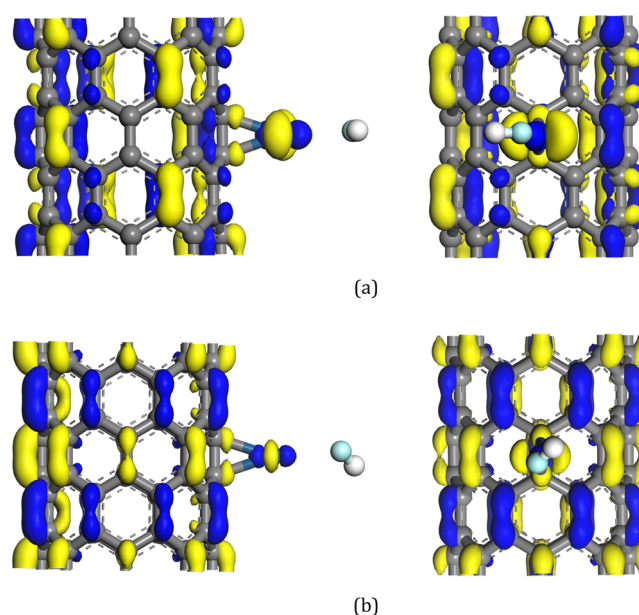
Figure 9. Configurations of the HOMO and LUMO of HF adsorbed on the Pt-SWCNT surface: (a) HOMO and (b) LUMO.

The overlap illustrates the hybridization between atomic orbitals.

The DOS distribution of COF_2 adsorbed on Pt-SWCNT is exhibited in Figure 7. It can be found that the TDOS has changed significantly after COF_2 adsorption and decrease obviously at the Fermi level. However, the hybridization between 2p orbitals of C, O, and F atoms in COF_2 and the 5d orbital of the Pt atom is slight according to the LDOS results.

3.3. Frontier Molecular Orbital Theory Analysis for HF, CS_2, and COF_2 Adsorbed on Pt-SWCNT. Frontier molecular orbital theory is investigated to better understand the Pt-SWCNT response to HF, CS_2, and COF_2. The distributions of the highest occupied molecular orbital (HOMO) and the lowest unoccupied molecular orbital (LUMO) accompanied by related energies are obtained and shown in Figures 8−11. Subsequently, the energy difference E_g = LUMO−HOMO, which could be a feasible parameter to measure the conductivity of materials.[34]
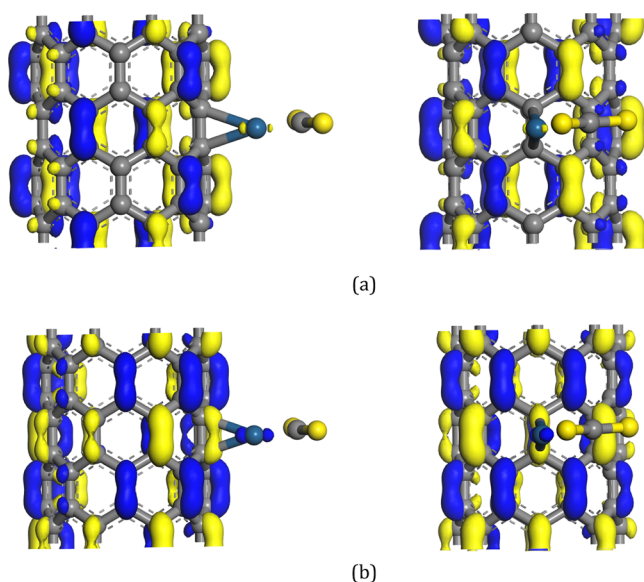
Figure 10. Configurations of the HOMO and LUMO of CS_2 adsorbed on the Pt-SWCNT surface: (a) HOMO and (b) LUMO.
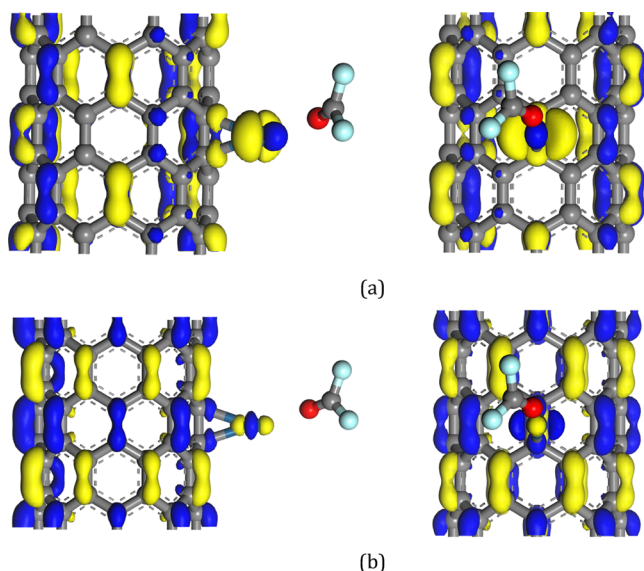
Figure 11. Configurations of the HOMO and LUMO of COF_2 adsorbed on the Pt-SWCNT surface: (a) HOMO and (b) LUMO.

The values of HOMO and LUMO are shown in Table 2. It can be found that both the HOMO and LUMO of isolated Pt-SWCNT are mainly around the tube and Pt has an E_g of 0.747 eV. For HF, CS_2, and COF_2 adsorption systems, all of the three gas molecules have little contribution to the HOMO and LUMO according to Figure 9−1011. However, the HOMO and LUMO areas around the Pt atom are obviously reduced after CS_2 adsorbed on Pt-SWCNT. In addition, E_g values of the three gas molecule adsorption systems have narrowed compared with that of isolated Pt-SWCNT, namely, 0.711 eV for the HF system, 0.693 eV for the CS_2 system, and 0.710 eV for the COF_2 system. This would lead to an increase in the conductivity of the Pt-SWCNT material interacting with the three kinds of gases in the order CS_2 > COF_2 ≈ HF. The result is consistent with the order of the response of the Pt-SWCNT surface to the three kinds of gases. This provides theoretical evidence for the detection of SF_6 decomposition components, HF, CS_2, and

COF_2, by a Pt-SWCNT-based sensor through the change in electrical conductivity.

4. CONCLUSIONS

In the work, the adsorption properties of HF, CS_2, and COF_2 on Pt-SWCNT have been studied based on DFT, including adsorption structure, binding energy, charge transfer, DOS, and frontier molecular orbital theory. The conclusions are summarized as follows.

(1) All processes of HF, CS_2, and COF_2 adsorbed on Pt-SWCNT are exothermic. After comprehensive consideration of binding energy and charge transfer, the response of Pt- SWCNT to CS_2 may be the best, and those to HF and COF_2 are almost the same.

(2) After the adsorption of the three kinds of gases on Pt-SWCNT, the order of the conductivity of the Pt-SWCNT material is CS_2 > COF_2 ≈ HF via frontier molecular orbitals theory analysis.

(3) The Pt-SWCNT material is probably more suitable as a gas sensor for the detection of CS_2 in the application of gas-insulated equipment.

■ ASSOCIATED CONTENT

ⓢ Supporting Information

The Supporting Information is available free of charge at https://pubs.acs.org/doi/10.1021/acsomega.1c02562.

All initial adsorption orientation configurations of HF, CS_2, and COF_2 adsorbing on Pt-SWCNT; adsorption parameters after optimization; and optimal molecular structures of HF, CS_2, and COF_2 (PDF)

■ AUTHOR INFORMATION

Corresponding Author

Gang WEI − *College of Electrical Engineering, Chongqing University of Science and Technology, Chongqing 401331, China;* ⓞ orcid.org/0000-0003-2182-8635; Email: eecqweig@163.com

Authors

Zhengqin CAO − *College of Electrical Engineering, Chongqing University of Science and Technology, Chongqing 401331, China;* ⓞ orcid.org/0000-0002-8274-629X

Xiaoyu WU − *College of Electrical Engineering, Chongqing University of Science and Technology, Chongqing 401331, China*

Gang HU − *College of Electrical Engineering, Chongqing University of Science and Technology, Chongqing 401331, China*

Qiang YAO − *State Grid Chongqing Electric Power Company, Chongqing 400015, China*

Haiyan ZHANG − *College of Electrical Engineering, Chongqing University of Science and Technology, Chongqing 401331, China*

Complete contact information is available at:
https://pubs.acs.org/10.1021/acsomega.1c02562

Notes

The authors declare no competing financial interest.

■ REFERENCES

(1) Shou, R.; Hata, K.; Nakano, M.; Suehiro, J. Chemical detection of SF_6 decomposition products generated by ac and dc corona discharges using a carbon nanotube gas sensor. *Adv. Mat. Res.* 2013, 699, 909−914.

(2) Cao, Z. Q.; Tang, J.; Zeng, F. P.; Yao, Q.; Miao, Y. L. SF_6 positive DC partial discharge decomposition components under four typical insulation defects. *IET Gener. Transm. Distrib.* 2019, 13, 1−8.

(3) Zhang, X. X.; Cui, H.; Chen, D. C.; Dong, X. C.; Tang, J. Electronic structure and H_2S desorption property of Pt_3 cluster decorated (8,0) SWCNT. *Appl. Surf. Sci.* 2018, 428, 82−88.

(4) Zhang, X.; Gui, Y.; Dong, X. Preparation and application of TiO_2 nanotube array gas sensor for sf_6-insulated equipment detection: a review. *Nanoscale Res. Lett.* 2016, 11, No. 302.

(5) Gui, Y.; Tang, C.; Zhou, Q.; Xu, L.; Zhao, Z.; Zhang, X. The sensing mechanism of N-doped SWCNTs toward SF_6 decomposition products: A first-principle study. *Appl. Surf. Sci.* 2018, 440, 846−852.

(6) Zhong, L.; Ji, S.; Liu, K.; Zhu, L.; Xiong, Q.; Cui, Y. Decomposition characteristics and mechanism of SF_6 under surface defect on solid insulator. *High Voltage Eng.* 2018, 44, 2977−2987.

(7) Zhong, L.; Ji, S.; Liu, K.; Xiong, Q.; Zhu, L. Decomposition characteristics of SF_6 under three typical defects and the diagnostic application of triangle method. *IEEE Trans. Dielect. Electr. Insul.* 2016, 23, 2594−2606.

(8) Zhang, X.; Cheng, Z.; Li, X. Cantilever enhanced photoacoustic spectrometry: quantitative analysis of the trace H_2S produced by SF_6 decomposition. *Infrared Phys. Technol* 2016, 78, 31−39.

(9) Zeng, F.; Tang, J.; Fan, Q.; Pan, J.; Zhang, X.; Yao, Q.; et al. Decomposition characteristics of SF_6 under thermal fault for temperatures below 400 °C. *IEEE Trans. Dielect. Electr. Insul.* 2014, 21, 995−1004.

(10) Cui, H.; Zhang, X.; Chen, D.; Tang, J. Pt & Pd decorated CNT as a workable media for SOF2 sensing: A DFT study. *Appl. Surf. Sci.* 2019, 471, 335−341.

(11) Gui, Y.; Wang, Y.; Duan, S.; Tang, C.; Zhou, Q.; Xu, L.; Zhang, X. Ab Initio Study of SOF_2 and SO_2F_2 Adsorption on Co-MoS_2. *Acs Omega* 2019, 4, 2517−2522.

(12) Gui, Y.; Liu, D.; Li, X.; Tang, C.; Zhou, Q. DFT-based study on H_2S and SOF_2 adsorption on Si-MoS_2 monolayer. *Results in Phys.* 2019, 13, No. 102225.

(13) Chen, Y.; Yin, S.; Li, Y.; Cen, W.; Li, J.; Yin, H. Curvature dependence of single-walled carbon nanotubes for SO_2 adsorption and oxidation. *Appl. Surf. Sci.* 2017, 404, 364−369.

(14) Cui, H.; Zhang, X.; Zhang, J.; Tang, J. Adsorption behaviour of SF_6 decomposed species onto Pd4-decorated single-walled CNT: a DFT study. *Mol. Phys.* 2018, 116, 1749−1755.

(15) Luna, C.R.; Bechthold, P.; Brizuela, G.; Juan, A.; Pistonesi, C. The adsorption of CO, O_2 and H_2 on Li−doped defective (8,0) SWCNT: A DFT study. *Appl. Surf. Sci.* 2018, 459, 201−207.

(16) Xiao, S.; Zhang, J.; Zhang, X.; Cui, H. Pt-doped single-walled CNT as a superior media for evaluating the operation status of insulation devices: a first-principle study. *AIP Adv.* 2018, 8, No. 105101.

(17) Yoosefian, M.; Etminan, N. The role of solvent polarity in the electronic properties, stability and reactivity trend of a tryptophane/Pd doped SWCNT novel nanobiosensor from polar protic to non-polar solvents. *RSC Adv.* 2016, 6, 64818−64825.

(18) Etminan, N.; Yoosefian, M.; Raissi, H.; Hakimi, M. Solvent effects on the stability and the electronic properties of histidine/Pd-doped single-walled carbon nanotube biosensor. *J. Mol. Liq.* 2016, 214, 313−318.

(19) Reinecke, T. L.; Perkins, F. K.; Robinson, J. A.; Snow, E. S.; BaDescu, C. Role of defects in single-walled carbon nanotube chemical sensors. *Nano Lett.* 2006, 6, 1747.

(20) Yoosefian, M. A high efficient nanostructured filter based on functionalized carbon nanotube to reduce the tobacco-specific nitrosamines, NNK. *Appl. Surf. Sci.* 2018, 434, 134−141.

(21) Peng, X.; Meguid, S. A. Molecular dynamics simulations of the buckling behavior of defective carbon nanotubes embedded in epoxy nanocomposites. *Eur. Polym. J.* 2017, 93, 246−258.

(22) Zhan, X.; Cui, H.; Chen, D.; Dong, X.; Tang, J. Electronic structure and H_2S adsorption property of Pt3 cluster decorated (8, 0) SWCNT. *Appl. Surf. Sci.* 2018, 428, 82−88.

(23) Penza, M.; Rossi, R.; Alvisi, M.; Cassano, G.; Signore, M. A.; Serra, E.; Giorgi, R. Pt- and Pd-nanoclusters functionalized carbon nanotubes networked films for sub-ppm gas sensors. *Sens. Actuators, B* 2008, 135, 289−297.

(24) Cui, H.; Zhang, X.; Zhang, J.; Ali Mehmood, M. Interaction of CO and CH_4 Adsorption with Noble Metal (Rh, Pd, and Pt)-Decorated N3-CNTs: A First-Principles Study. *ACS Omega* 2018, 3, 16892−16898.

(25) Yoosefian, M.; Zahedi, M.; Mola, A.; Naserian, S. A. DFT comparative study of single and double SO_2 adsorption on Pt-doped and Au-doped single-walled carbon nanotube. *Appl. Surf. Sci.* 2015, 349, 864−869.

(26) Delley, B. From molecules to solids with the DMol3 approach. *J. Chem. Phys.* 2000, 113, 7756−7764.

(27) Li, T.; Gui, Y.; Zhao, W.; Tang, C.; Dong, X. Palladium modified MoS_2 monolayer for adsorption and scavenging of SF_6 decomposition products: A DFT study. *Phys. E.* 2020, 123, No. 114178.

(28) Cao, Z.; Wei, G.; Zhang, H.; Hu, D. W.; Yao, Q. Adsorption Property of CS_2 and COF_2 on Nitrogen-Doped Anatase TiO_2 (101) Surfaces: A DFT Study. *ACS Omega* 2020, 5, 21662−21668.

(29) Zhang, X.; Gui, Y.; Xiao, H.; Zhang, Y. Analysis of adsorption properties of typical partial discharge gases on Ni-SWCNTs using density functional theory. *Appl. Surf. Sci.* 2016, 379, 47−54.

(30) Li, K.; Wang, W.; Cao, D. Metal (Pd, Pt)-decorated carbon nanotubes for CO and NO sensing. *Sens. Actuators, B* 2011, 159, 171−177.

(31) Zhang, X.; Lei, Y.; Jing, T.; Dong, X. Gas Sensitivity and Sensing Mechanism Studies on Au-Doped TiO_2 Nanotube Arrays for Detecting SF_6 Decomposed Components. *Sensors* 2014, 14, 19517−19532.

(32) Chen, W.; Gui, Y.; Li, T.; Zeng, H.; Xu, L.; Ding, Z. Gas-sensing properties and mechanism of Pd-GaNNTs for air decomposition products in ring main unit. *Appl. Surf. Sci.* 2020, DOI: 10.1016/j.apsusc.2020.147293..

(33) Xiao, S.; Zhang, J.; Zhang, X.; Cui, H. Pt-doped single-walled CNT as a superior media for evaluating the operation status of insulation devices: A first-principle study. *AIP Adv.* 2018, 8, No. 105101.

(34) Karami Horastani, Z.; Hashemifar, S. J.; Sayedi, S. M.; Sheikhi, M. H. First principles study of H_2 adsorption on the pristine and oxidized (8,0) carbon nanotube. *Int. J. Hydrogen Energy* 2013, 38, 13680−13686.

(35) Gilje, S.; Han, S.; Wang, M.; Wang, K. L.; Kaner, R. B. A chemical route to graphene for device applications. *Nano Lett.* 2007, 7, 3394.